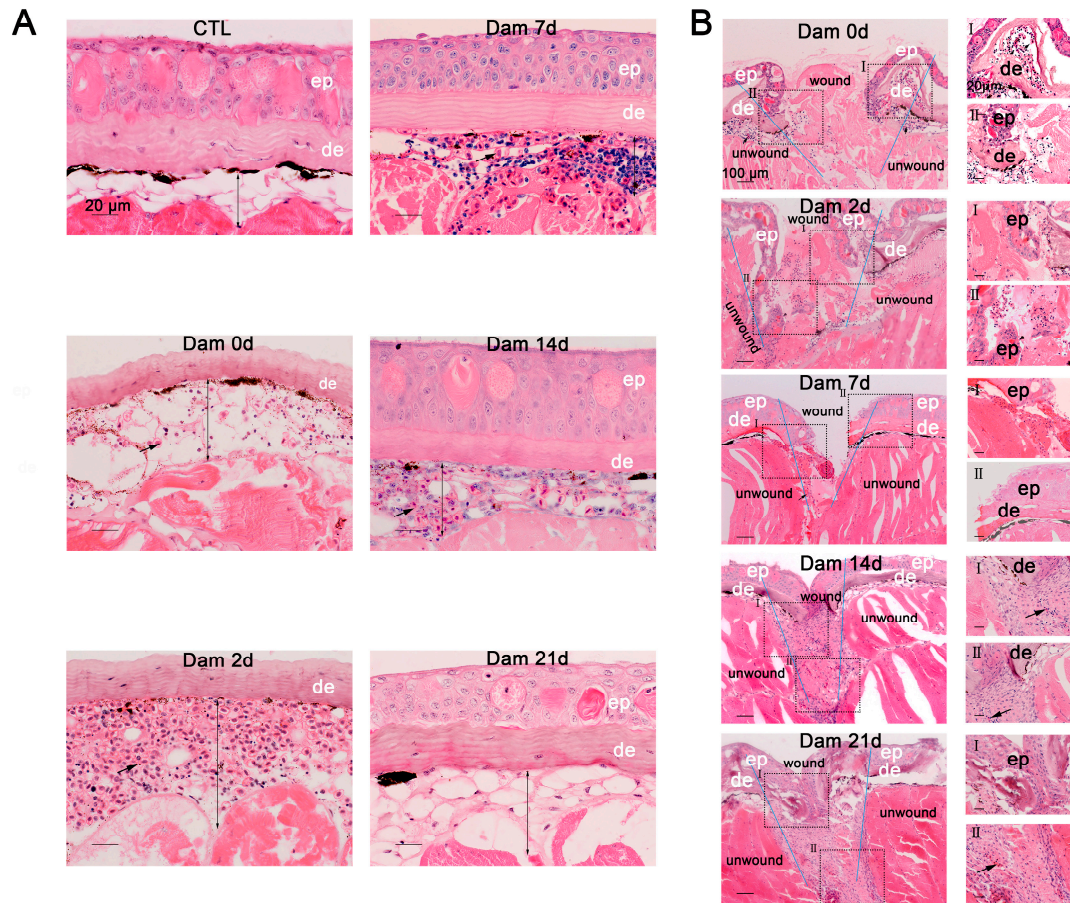
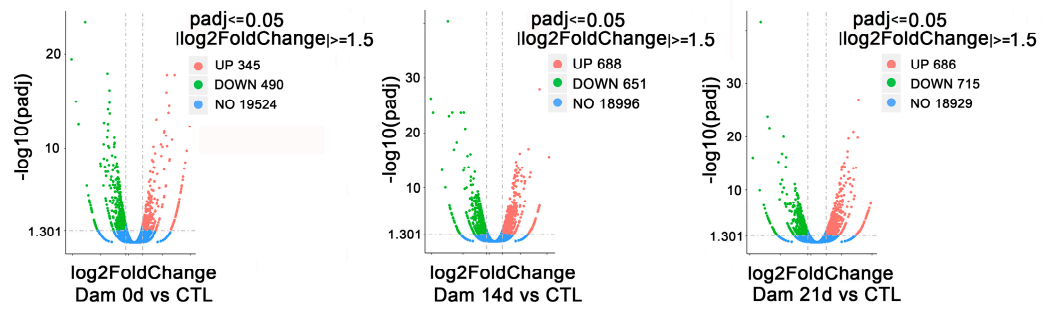


Supplementary Figure S1. Process of wound healing in lamprey. (A) Photograph of epidermal damage in larvae. From undamaged skin to 21 d after damage, hyperemia was more prominent; scale bars, 1000 μ m. (B) Photograph of full-thickness skin damage to lamprey larva, from undamaged skin to 21 d after damage, with repair delays; scale bars, 1000 μ m.

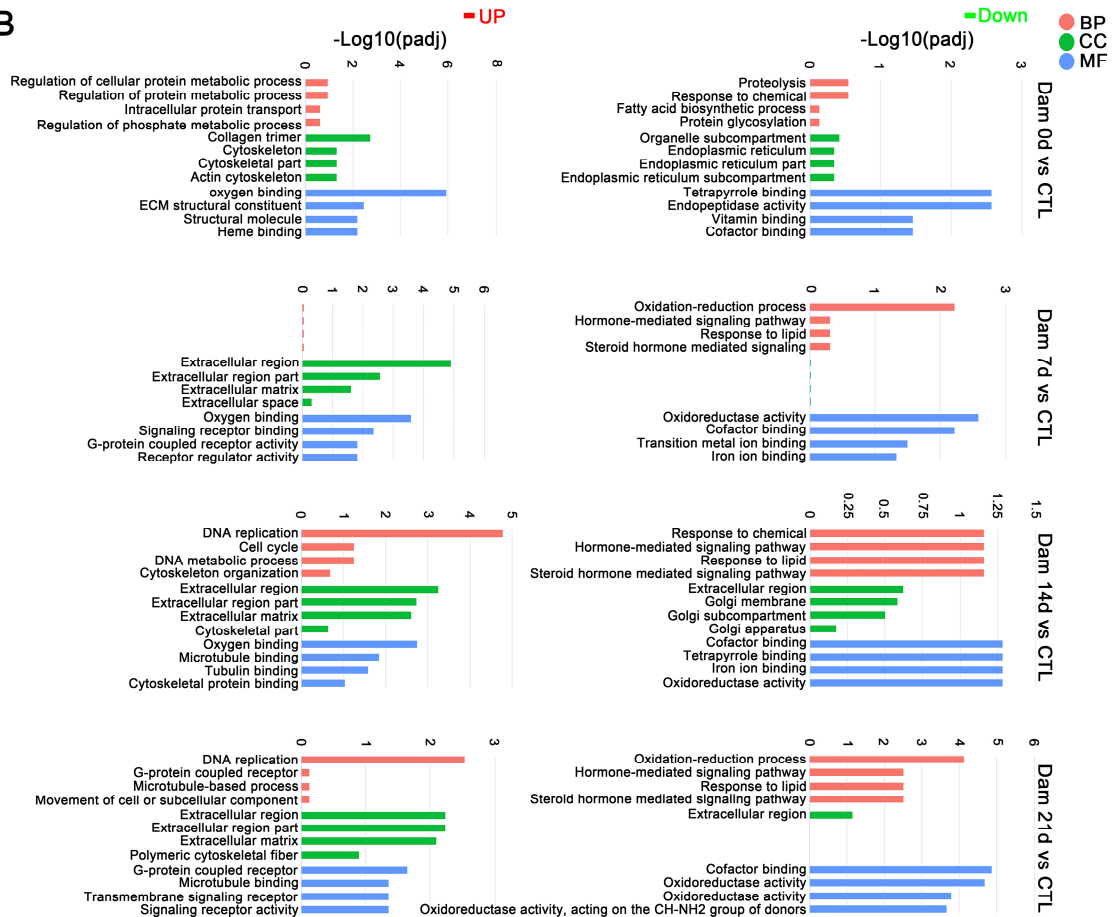


Supplementary Figure S2. H&E staining at all stages of skin damage. (A) Representative images of the skin healing process of larval lamprey after epidermal damage and RBC infiltration (black arrow). (B) Representative images of the skin healing process of larval lamprey after full-thickness skin damage. Deepening of the damage causes the repair process to be delayed. The right panel is a magnified view of the left panel.

A



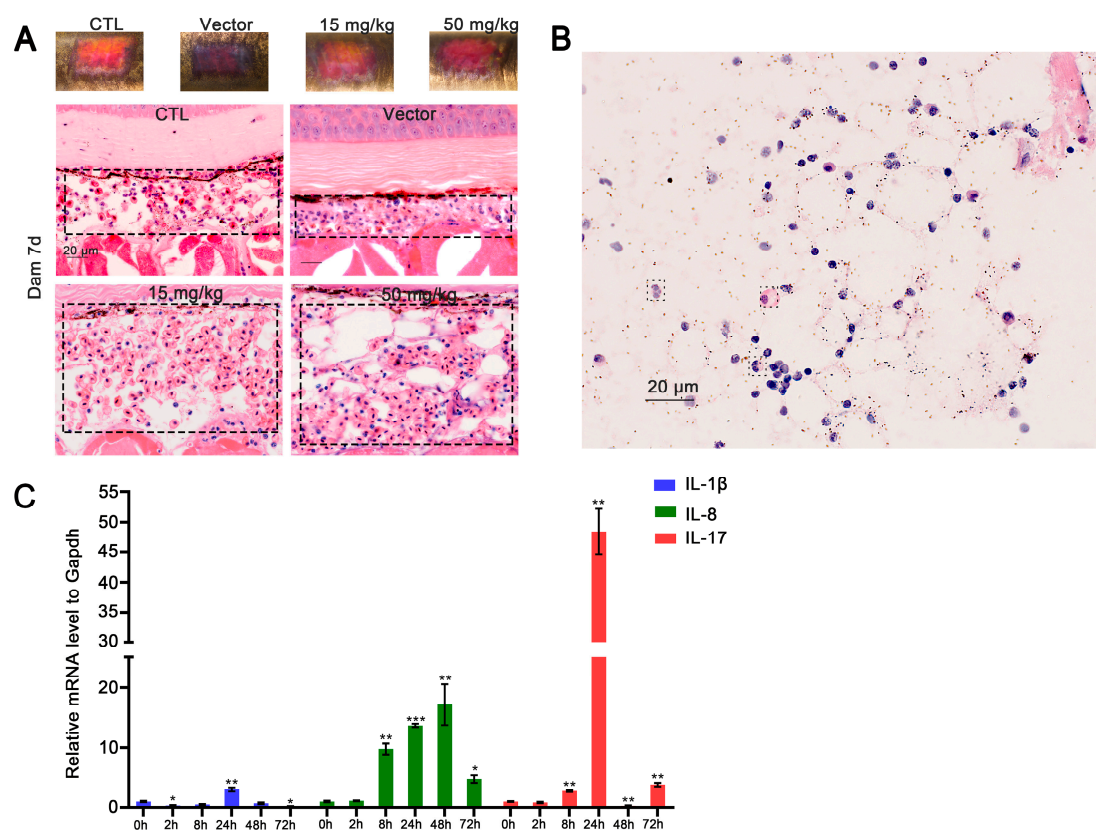
B



Supplementary Figure S3. RNA-seq results of skin tissue after epidermal damage in lamprey. (A) Volcano plot of the differentially expressed genes in lamprey after skin damage at all five time points. (B) GO functional category analysis of all five time points (from 0 d-21 d vs. CTL), showing upregulated DEGs (left) and downregulated DEGs (right).



Supplementary Figure S4. RNA-seq results of skin tissue after epidermal damaged in lamprey. KEGG analysis of all five time points (from Dam 0 d-21 d vs. CTL). The left side shows the upregulated DEGs, and the right side shows the downregulated DEGs. GB: Glycosphingolipid biosynthesis; CS: chondroitin sulfate.



Supplementary Figure S5. (A) Effect of RAC1 inhibitor addition on epidermal repair. Dam 7 d after addition of the Ehop-016 inhibitor. Early hypodermis changes were relieved on Dam 7 d (black box). Scale bars, 20 μ m. (B) Hypodermis smear of epidermal damage and different types of cell infiltration (black box). (C) Isolated RBCs stimulated by *Vibrio anguillarum* can promote inflammation. * $p < 0.05$, ** $p < 0.01$, *** $p < 0.001$.